

VISCOELASTIC PROPERTIES OF WET CORTICAL BONE—II. RELAXATION MECHANISMS*†

RODERIC S. LAKES

U. WISCONSIN

and

J. LAWRENCE KATZ

Center for Biomedical Engineering, Rensselaer Polytechnic Institute, Troy, NY 12181, U.S.A.

Abstract—The contributions of thermoelastic coupling and fluid motions to viscoelastic response in bone are calculated, using the theories of Zener and Rusch, respectively. Fluid motion and homogeneous thermoelasticity produce mechanical losses which are size dependent. Inhomogeneous thermoelastic coupling results in thermal currents between regions of different stiffness, such as osteons and lamellae, and around voids. Losses of this type display no size effect. Fluid motion, homogeneous thermoelasticity, and inhomogeneous thermoelasticity resulting from stiffness variations, yield losses which are significant enough to be measurable. An expression is derived for the contribution of piezoelectric-like coupling to the mechanical loss. This loss is calculated from published data, and for dry bone it is negligibly small. The role of inhomogeneous deformation and molecular modes in collagen as viscoelastic mechanisms is considered and experimental evidence is discussed.

INTRODUCTION

Compact bone has proven to be a highly complex material. It is inhomogeneous, anisotropic (Lang, 1970; Yoon and Katz, 1976), viscoelastic (see e.g. Rauber, 1876; Lakes *et al.*, 1979) and exhibits detailed structure on all levels of scale (see e.g. Hancox, 1972). The complex structure of bone has suggested to many investigators that an understanding of the physical properties, and in particular the mechanical properties, of bone can be arrived at via examination of its structure and the (markedly different) properties of its constituents.

When a viscoelastic solid is subjected to mechanical strain, part of the strain-energy is converted to other forms and ultimately degraded into heat. What happens to this energy in living bones can be of considerable biological importance. For example, bone is known to remodel itself in response to mechanical stress in such a way as to more effectively support the stress (Wolff's law). A variety of mechanisms have been proposed to account for this activity: (1) lamellar

motions; impingement on osteocyte processes (Tischendorf, 1951); (2) stress-induced fluid motion, resulting in improved nutrition of osteocytes (Mouradian, 1973; Renton, 1970) (3) Stimulation of bone cells by means of stress generated potentials (Bassett, 1964, 1965). Currently, the third of these is now considered by many as the possible origin of Wolff's law activity. In all the above processes, mechanical energy is transformed into other forms before being dissipated. An investigation of these and other viscoelastic mechanisms, in particular of their frequency dependence, can elucidate the role of strain energy dissipation in living tissues.

Among the large number of physical processes which are capable of causing viscoelastic‡ effects, the following shall be considered in the present study:

- (1) Thermoelastic coupling
 - a. Homogeneous effect
 - b. Inhomogeneous effect;
- (2) Piezoelectric-like coupling;
- (3) Motion of fluid in canals in bone;
- (4) Inhomogeneous deformation
 - a. Motion of osteons at cement lines
 - b. Motion of lamellae in osteons and interstitial lamellae
 - c. Motion of fibers within a lamella;
- (5) Molecular modes in collagen.

The mechanical damping resulting from the first three of these can be evaluated quantitatively. This is done in the following analysis.

RELAXATION DUE TO THERMOELASTICITY

Homogeneous effect

The stiffness measured for a solid is dependent upon

* Received 22 August 1977.

† This paper is based on part of a dissertation submitted by R. S. Lakes, while an N.I.H. Predoctoral Trainee, in partial fulfillment of the requirements for the Ph.D. in Physics at Rensselaer Polytechnic Institute.

‡ Viscoelastic effects are here taken to include any process which results in energy dissipation in mechanical deformation at small strains, and which does not permanently alter the structure of the material, regardless of cause. Several of the effects considered here depend on specimen size and are not included in the traditional study of viscoelasticity theory; nevertheless they result in macroscopically observable damping and hence must be included in the analysis of bone's behavior.

whether the measurement is performed under adiabatic or isothermal conditions. If the observation is done at frequencies at which the solid behaves neither adiabatically nor isothermally, a frequency dependence of the stiffness will be observed, as well as mechanical damping resulting from the irreversible flow of heat between the specimen and its (isothermal) environment. The adiabatic and isothermal compliance tensors S_{ijkl}^S and S_{ijkl}^T , respectively, are related by the following (Nye, 1957):

$$S_{ijkl}^S - S_{ijkl}^T = -\alpha_{ij}\alpha_{kl} \frac{T}{C^\sigma}, \quad (1)$$

where α is the thermal expansion tensor, T the absolute temperature and C^σ the heat capacity per unit volume at constant stress.

Observe that in a principal coordinate system in which α is diagonal, the difference between the adiabatic and isothermal shear compliances (such as S_{2323}) is zero, so that for shear deformation in such a system, there is no relaxation due to homogeneous thermoelasticity.

For a hypothetical experiment done in uniaxial tension or compression, in which the material axes of the specimen are oriented so that S_{3333} can be measured, the compliances differ. The frequencies at which the maximum energy loss occurs depend on the geometry:

$$\tan \delta_{ijkl}(\omega) = \Delta_{ijkl} \sum_n F_n \frac{\omega \tau_n(ijkl)}{1 + \omega^2 \tau_n^2(ijkl)}$$

with

$$\sum_n F_n = 1 \quad (2)$$

and $\Delta_{ijkl} = (S_{ijkl}^S - S_{ijkl}^T)/S_{ijkl}$, and F_n and τ_n are solutions of an eigenvalue problem for the geometry in question (Zener, 1938). For a circular cylinder of radius r in compression along the long axis, Zener has obtained $F_n = 4/q_n^2$, $\tau_n = \frac{r^2 C_v}{q_n^2 K}$, where C_v is the specific heat, K the thermal conductivity, and q_n the n 'th zero of the zero'th Bessel Function J_0 . For a bone specimen $\frac{1}{8}$ in. in diameter at body temperature, using the values for S , α , and K compiled in Table 1, and the specific heat for hydroxyapatite in the absence of a value for bone, the following is obtained:

Table 2. Homogeneous thermoelastic modes

n	q_n	$\tau_n(\text{sec})$	F_n	$F_n \Delta$	$\nu_n(\text{Hz})$
1	2.404	12	0.693	0.0014	0.013
2	5.520	2.3	0.131	0.0003	0.069
3	8.654	0.94	0.051	0.0001	0.169

Note that $F_n \Delta$ represents the peak value of $\tan \delta$ due to each mode and $\nu_n = 1/2\pi\tau_n$, the frequency at which that peak occurs.

While these values of $\tan \delta$ in tension or compression are real in the sense that they represent an actual energy loss, the relaxation is not intrinsic, in that the

characteristic times τ_n depend on the size of the specimen and their distribution depends on the shape of the specimen.

Inhomogeneous effect

Stress inhomogeneities in a solid which is subjected to dynamic loading give rise to fluctuations in temperature and therefore to heat flow between the inhomogeneities. This heat flow represents an irreversible conversion of mechanical energy to heat.

By means of thermodynamic arguments, it is possible to show that the loss tangent due to inhomogeneous thermoelastic relaxation is given by the following (Zener, 1938):

$$\tan \delta = \frac{\beta^2 T}{C_v X} R \sum_k F_k \frac{\nu_k \nu}{\nu_k^2 + \nu^2}; \quad \sum_k F_k = 1, \quad (3)$$

where β is the volume coefficient of thermal expansion, T the (absolute) temperature, C_v the heat capacity at constant volume per unit volume, and R is the fraction of strain-energy associated with dilatation. The characteristic frequencies ν_k and weighting coefficients F_k are obtained from analysis of the specific geometry in question.

The quantity $\Delta = \beta^2 T/C_v X$ represents an upper bound for the loss in a given material, since $R \leq 1$. For compact bone, this expression may be evaluated using the data in Table 1 and recognizing that the volume expansion coefficient β is given in terms of the linear expansion coefficients α by $\beta = \alpha_1 + \alpha_2 + \alpha_3$. The compressibility may be expressed in terms of the elastic constants by $X = S_{1111} + S_{2222} + S_{3333} + 2(S_{1122} + S_{2233} + S_{1133})$. The heat capacity used in the calculation is again that of hydroxyapatite in the absence of a value for whole bone. For bone at body temperature, then, $\Delta = 8.1 \times 10^{-3}$.

In order to evaluate the quantity R , a stress analysis must be performed on the inhomogeneities in question. Zener (1938) obtains values for R corresponding to inhomogeneous stress in the randomly oriented, anisotropic, cubic crystals of a polycrystalline metal. The largest value for R so obtained was 0.065 for lead. Now, in bone, the variation in stiffness among osteons results from differences in structure as well as degree of calcification. Ascenzi and Bonucci (1966) have observed differences as great as a factor of 2 in the Young's modulus of different types of osteons. This greatly exceeds the variation in stiffness of the crystallites of lead due to random orientation. Therefore, the value of R for bone is likely to be significantly greater than that for lead, but it could not be expected to attain the upper bound of 1 corresponding to pure local dilatation. To calculate R explicitly for bone, the anisotropy of the different types of osteons and lamellae must be known. Lacking this information, only an upper bound on the relaxation strength, corresponding to $R = 1$, can be given.

The characteristic frequency ν_0 of these thermoelastic losses, that is, the frequency at which $\tan \delta$ is maximum, depends only on the thermal relaxation

Table 1. Some relevant physical properties of bone

Substance	Property	Value	Units	Conditions	Reference
Human bone	Volume fraction of (i) canaliculi	1.48	%		Frost (1960)
	(ii) lacunae	0.80	%		
Human femur	Cross-section area of spaces	6.1	%		Evans and Bang (1966)
Human fibula	Thermal expansion, α	2×10^{-5}	$^{\circ}\text{C}$	Parallel to bone axis	Liboff and Shamos (1973)
		3×10^{-5}	$^{\circ}\text{C}$		
Human tibia	Thermal conductivity	7.1×10^{-4}	joule/K/cm/sec	Wet	Hamill and Harper (1975)
Hydroxyapatite Bone	Heat capacity, c_p	770.52	joule/mol/K	$T = 298.16 \text{ K}$	Egan <i>et al.</i> (1971)
	Piezoelectric coefficients, d_{123}	0.130	pcoul/Nt	Dry	Liboff <i>et al.</i> (1971)
		-0.203	pcoul/Nt		
	Bone	Dielectric constant, K'_{11}	5.9	—	Dry bone
Dielectric loss, K''_{11}		0.1	—	1-100 kHz	
Human bone	Compliance, S_{2323}	11.48×10^{-11}	$\frac{\text{M}^2}{\text{Nt}}$	Dry, ultrasonic	Yoon and Katz (1976)

time for heat flow between the inhomogeneities (of size L) in question. v_o is given by $v_o = k/L^2 C_v$, where k is the thermal conductivity, C_v the heat capacity and L is the thermal path length.

The presence of cavities in a solid also gives rise to a relaxation of thermoelastic origin,† as a result of inhomogeneous stress distributions around the cavities. For spherical cavities in an isotropic solid subjected to shear

$$R = \frac{10}{1764} VP(N),$$

where

$$P(N) = (1 - 2N) \left(1 - \frac{5N}{7}\right)^2.$$

V is the volume fraction of cavities and N is Poisson's ratio (Zener, 1938). For compact bone, $N = 0.34$, so that $R = 4 \cdot 10^{-3} \cdot V$. Calculated values for R and for the maximum value of $\tan \delta$ are presented in Table 3.

The distribution of frequencies associated with this relaxation is given by

$$F(x) = \frac{18x^2}{x^6 - 2x^4 + 9x^2 + 81},$$

where the sum

$$\sum_k F_k \frac{v_k v}{v_k^2 + v^2}$$

in equation (3) is replaced by the integral

$$\int_0^\infty F(x) \frac{v(x)v}{v^2(x) + v^2} dx.$$

$$v(x) = \left(\frac{k}{2C_v \pi r^2}\right) x^2,$$

where r is the cavity radius.

It should be noted that, although anisotropy has been neglected for the case of cavities (since the local anisotropy is not known), the peak value of $\tan \delta$ could in no case exceed $V \cdot \Delta$. The actual lacunae are ellipsoidal, and the actual osteons are cylindrical in shape, therefore the assumption of spherical cavities leads to an approximate result. In view of the smallness of the predicted loss, more sophisticated modelling was not undertaken. Viscoelastic response due to stiffness variations, in contrast, could be large enough to detect, if the value of R approached the theoretical upper bound of 1. An explicit calculation of R would be very complex and would require micromechanical data which are presently unavailable.

The ratio of the stiffness of apatite to that of collagen is at least 100, considerably greater than the stiffness variation among osteons. Due to the small size of the apatite crystallites, the characteristic frequency of the

inhomogeneous thermoelastic relaxation is well above the range of physiologic interest and therefore is not included here.

Calculated mechanical losses due to inhomogeneous thermoelastic effects show no dependence on the size or shape of the specimen. This will be true provided that the smallest dimension of the specimen is much larger than any of the inhomogeneities considered.

RELAXATION DUE TO STRESS-GENERATED POTENTIALS

The stiffness of an elastic crystal is increased by the presence of piezoelectric coupling. By the use of thermodynamic arguments (Nye, 1957), it is possible to show that the difference between the compliance at constant electric displacement S_{ijkl}^D and the compliance at constant electric field S_{ijkl}^E is given by

$$S_{ijkl}^D - S_{ijkl}^E = -d_{nij} d_{mkl} (k_{mn})^{-1}, \quad (4)$$

where d is the piezoelectric modulus tensor, k is the dielectric tensor at constant stress, and the temperature is assumed to be constant.

If the material in question is semiconducting, or exhibits dielectric relaxation, and is subjected to a transient (step-function) stress, the stress generated polarization will be neutralized after a period of time. Electrical energy will have been dissipated, resulting in a relaxation of the mechanical stress.

Mechanical losses induced by stress-generated potentials, as well as the piezoelectric-like stiffening referred to above, may be expected to depend upon the electrical boundary conditions imposed on the specimen. Therefore, consider a specimen in the shape of a thin plate, oriented so that the 1 axis is perpendicular to its surface. Now the constitutive equation for a linear piezoelectric-like solid is

$$D_n = d_{nij} \sigma_{ij} + k_{nm} E_m. \quad (5)$$

For lossy materials, the coefficients d and k may be considered to be complex:

$$d^* = d' - id''; \quad k^* = k' - ik''. \quad (6)$$

Now from Gauss's law, the boundary condition on the electric displacement D is $D_{in}^{[normal]} - D_{out}^{[normal]} = \Sigma_{free}$, where Σ_{free} is the density of free charge on the surface. Since for the geometry in question $D_{out}^{[normal]} = 0$, $D_{in}^{[normal]} = \Sigma_{free}$. The current density $J_n = (d/dt)\Sigma_{free}$, is related to the electric field by the dynamic conductivity $g_{nm}^{(\omega)}$: $J_n = g_{nm} E_n$. However, since $g_{nm} = k_{nm}'' \cdot \omega$, one is left with $i\omega D_m^{[normal]} = k_{mn}'' \omega E_n$, or $D_1 = -ik_{1n}'' E_n$. If it is assumed that k is diagonal in the chosen coordinate system, then $E_1 = (i/k_{11}'') D_1$.

As shown in Appendix A, the mechanical loss due to weak piezoelectric coupling is given by equation (A-12):

$$\Delta \tan \delta_{2323}^{Mech} = \frac{d_{123}^2 - d_{123}''^2}{k_{11}' S_{2323}'} \tan \delta_{11}^{(k)}, \quad (7)$$

where $\tan \delta_{11}^{(k)}$ is the dielectric loss tangent.

† This comes from the transfer of heat generated by the coupling described above. This relaxation must be distinguished from that resulting from redistribution of stresses among viscoelastic phases near a stress concentration.

Table 3. Inhomogeneities in bone and associated thermoelastic losses

Type of inhomogeneity, cavity	Dimension, $r(\mu\text{m})$	V	R		$\nu_0(\text{Hz})$	$\tau_0(\text{sec})$
			$0.004 V$	$R\Delta = \tan \delta \text{ max}$		
lacunae	8	0.008	3.2×10^{-5}	2.6×10^{-7}	18	0.009
Haversian Canals	35	0.05	2.0×10^{-4}	1.6×10^{-6}	1.2	0.13
canaliculi		0.015	6.0×10^{-5}	4.9×10^{-7}		
Stiffness	$d(\mu\text{m})$			Δ	$\nu_0(\text{Hz})$	$\tau_0(\text{sec})$
osteons	300				0.063	2.53
osteons	200			0.0081	0.14	1.14
lamellae	20				0.44	0.35

For 'dry' bone, the piezoelectric-like coefficients for shear, d_{123} , d_{213} , greatly exceed those for compression. Using the published values for the properties of compact bone, which are collected in Table 3, the piezoelectric-like contribution to the loss becomes $\Delta \tan \delta_{2323} = 5 \times 10^{-8}$. The contribution $\Delta \tan \delta_{1313}$ is somewhat larger: 1.2×10^{-7} . This is far too small to be resolved above other losses, typically of the order 10^{-2} in bone; however, it must be recognized that the electrical properties of bone are dependent on frequency, humidity and temperature. Values for the complex piezoelectric-like coefficients as functions of frequency have only just recently appeared in the literature (Bur, 1976; Pfeiffer, 1977).

Relaxation due to an inhomogeneous piezoelectric-like effect, in which stress-related polarizations are generated and annihilated locally, is conceivable, given the structure of bone. No experimental data on such an effect appear to be available.

RELAXATION DUE TO FLUID MOTION

A sizeable fraction of the volume of even compact bone consists of voids. A dissipation of mechanical energy can result from the motion of fluids in connected voids, if the strain applied produces a volume change and if the specimen has a free surface. Strain-induced fluid-motion has been suggested as a mechanism for certain elements of the 'piezoelectric-like' tensor of wet bone (Anderson and Eriksson, 1970) and for facilitated transport of nutrients to, and wastes from, osteocytes.

An explicit calculation of the contribution of fluid-motion to the viscoelastic response of porous materials (foams) has been done by Rusch (1965). The following expression is obtained for the loss tangent for tension/compression along the 3 axis of a solid containing pores filled with an incompressible fluid of viscosity η :

$$\tan \delta = \{d_0[1 + \beta^2(\gamma_r/8)^2] + (\gamma_r/12)\} / [1 + \beta^2(\gamma_r/8)^2 + \beta(\gamma_r/8)^2], \quad (8)$$

where $\beta = 2(E_3/E_1)(h/r)^2$, $\gamma_r = \omega\eta r^2/\phi E_3 K$, d_0 is $\tan \delta$ for the matrix alone, h and r are the length and radius, respectively, of the cylindrical specimen, E_3 and E_1 the

Young's modulus in the longitudinal and transverse directions, respectively, of the matrix alone (no fluid in pores), ϕ the volume fraction of pores and K the permeability of the specimen. K can be taken as a constant, provided the flow velocity of fluid is small and the channels not too irregular. The small-strain assumption used in the analysis is satisfied in the regime of viscoelastic behavior in bone. The constant K may be expressed approximately as $K = (C/\tau)(\phi/S)^2$, where C is a constant depending on the tube cross section, lying between 0.5 and 0.6 for circular, square and triangular cross section; τ is the tortuosity or flow path length divided by total path length and S is the surface area of interconnecting pores divided by their volume. For an array of parallel cylindrical tubes of diameter d , $K = d^2\phi^2/32$; however, for bone, Haversian canals and Volkmann's canals run at right angles, so we take $\tau = \sqrt{2}$, whence $K = d^2\phi^2/32\sqrt{2}$.

The calculation of the fluid-flow contribution to $\tan \delta$ for bone is done using the following values:

$$\begin{aligned} \phi &= 0.1 \\ E_3 &= 2.74 \times 10^{10} \text{ Nt/m}^2 \text{ (from compliances measured} \\ E_1 &= 1.88 \times 10^{10} \text{ Nt/m}^2 \text{) by Yoon and Katz, 1976)} \\ d &= 20 \mu\text{m} = 2 \times 10^{-5} \text{ m} \\ h &= 1 \text{ in.} = 2.54 \times 10^{-2} \text{ m (typical specimen} \\ &\quad \text{dimensions)} \\ r &= 1/16 \text{ in.} = 1.59 \times 10^{-3} \text{ m} \\ d_0 &= 0.01 \\ \eta &= 10^{-2} \text{ poise} = 10^{-3} \text{ MKS (water).} \end{aligned}$$

The results of this calculation are shown in Fig. 1. It should be noted that the loss-tangent due to this mechanism would peak at 1000 Hz if the anisotropy in porosity were not considered. Since the fluid-flow permeability tensor for bone has not, to the authors' knowledge, been published, several longitudinal sections of bovine bone were studied under the microscope. The number of channels piercing these sections (radial direction) were counted and their average size estimated, yielding a permeability of $3.16 \times 10^{-16} \text{ m}^2$ in the transverse (radial) direction. This value was used in the calculation.

The problem of fluid-flow damping in bone has been

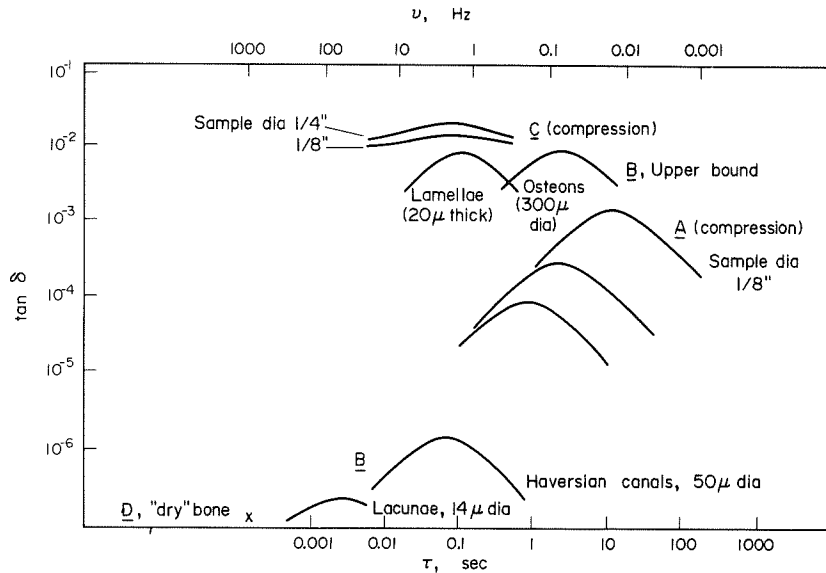


Fig. 1. Contributions of several relaxation mechanisms to the loss tangent of cortical bone: A. Homogeneous thermoelastic effect; B. Inhomogeneous thermoelastic effect; C. Fluid flow effect; D. Piezoelectric effect.

approached by Mouradian (1973) who has, using Rusch's theory, calculated the loss due to a compressible fluid using the bulk modulus of air, rather than that of water. Moreover, Mouradian did not note the dependence of the fluid-flow loss on specimen size and shape. Water has been treated as incompressible in the present study, since its compressibility is less than one-tenth that of dry bone.

The preceding arguments depend on the assumption that a volume change occurs in the solid portion of the bone. For the case of torsion about the symmetry axis of an axisymmetric solid, there is no overall volume change and hence no energy dissipation due to this type of fluid motion. Local volume changes due to the inhomogeneity of bone may cause some damping, but this would be difficult to assess; the magnitudes of $\tan \delta$ calculated for tension/compression would represent an upper bound. Loss due to the shear of water in the absence of bulk transport is entirely negligible, since the shear stress in water does not approach that in bone until a frequency of 10^{12} Hz is reached.

INHOMOGENEOUS DEFORMATION

Microscopic examination of bone fracture surfaces has revealed that slowly moving cracks, in particular, tend to propagate along the cementing lines (Piekariski, 1970). This observation has led some authors to postulate that the 'cement-line' material, primarily composed of protein-polysaccharides, behaves as a 'zone of weakness' and acts to retard some types of fracture and accelerate others. If this material exhibits a large compliance or is in fact viscous at small macroscopic stresses, then motion along these interfaces can result in large mechanical relaxations.

In polycrystalline metals, a similar mechanism, slippage along the grain boundaries, can be shown to cause a relaxation of about 40% of the initial stress in a

stress relaxation experiment (Zener, 1941). The central assumptions in this analysis were: (i) grains are modelled as interlocking polyhedra; (ii) the boundaries are viscous, hence the shear stress across them vanishes in the relaxed state. Experimentally, it is observed that such large, recoverable relaxations do occur in metals (Kê, 1947); at room temperature the characteristic time can be many days.

The complex geometry of the microstructure of bone, including branchings and interconnections of osteons, has thus far precluded any attempt to theoretically evaluate the relaxation strength associated with inhomogeneous deformation. Experimental observation of the lamellae of human bone specimens subjected to stress in cantilever bending has been done by Tischendorf (1951). Displacements at the boundaries between lamellae were noted, and were found to increase with time following the application of load; however the time scale associated with this motion was not specified.

DISCUSSION

The contributions of several physical processes to viscoelastic response in bone in compression and in shear have been plotted in Fig. 1. The loss tangent in bone in shear is typically $\sim 10^{-2}$ over the domain 0.1–100 Hz (Lakes *et al.*, 1979). Homogeneous thermoelastic coupling, as well as fluid flow effects (to first order), contributes nothing to losses in shear. Inhomogeneous thermoelastic effects, in contrast, could result in measurable losses, provided that the resolution in the experimental apparatus is adequate. Relaxation spectra obtained from the torsional viscoelastic data presented in Part 1 are suggestive of a possible role of inhomogeneous thermoelasticity as a contributing mechanism for losses at times from 0.1 to 10 sec (Figs. 2

and 3). The differentiation process used to obtain the spectra from the measured properties has increased the scatter in the points. The curves were fitted by eye, since there was no *a priori* reason to prefer a particular analytical form. Despite the scatter, the spectrum in Fig. 2 does not appear to be monotonically increasing with $\log t$; rather, there appear to be variations in slope, or 'humps' in the curve. The 'humps' in the relaxation spectra for human bone (Fig. 2) at ~ 9 sec, 0.3 sec and 0.02 sec would correspond to inhomogeneity sizes of 560, 103 and 27 μm , respectively, if they were caused by this mechanism. There is some un-

certainty in these values, since the specific heat of apatite was used, rather than that for bone. The 560 μm dimension is larger than that of a typical osteon by a factor of about 2.5. The 103 μm dimension may be associated with thermal diffusion between the inner lamellae of an osteon and the material within its Haversian canal. The 27 μm dimension is larger than that of typical lamellae by a factor of approximately 4. Although the lamellae are about 7.5 μm thick (Frost, 1963), Frasca (1974) has suggested that the relevant structural unit may be several times thicker. Specifically, fibers in groups of several adjacent lamellae were

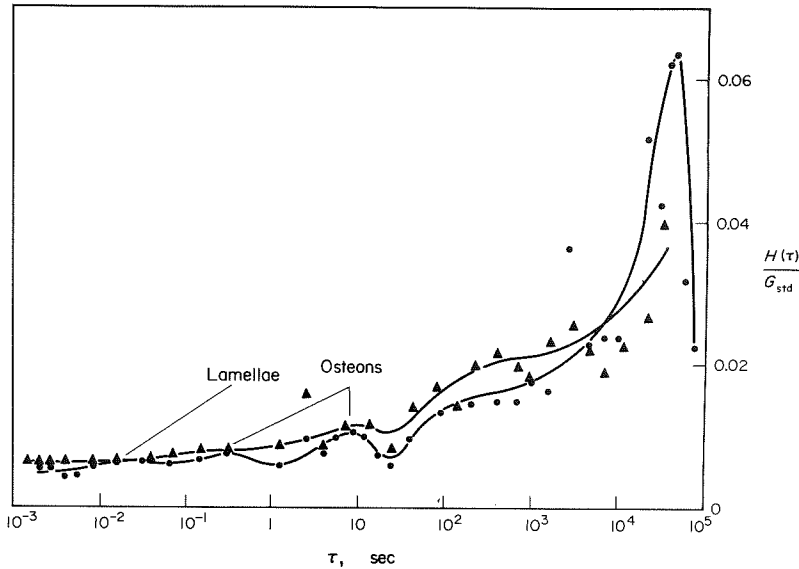


Fig. 2. Comparison of relaxation spectra for wet human bone, specimens 5 and 6 (Lakes *et al.*, 1979) in simple torsion; $T = 37^\circ\text{C}$. First approximation from relaxation and dynamic data. ● Human tibial bone, specimen 6. ▲ Human tibial bone, specimen 5. $G_{\text{std}} = G(10 \text{ sec})$. $G_{\text{std}}^{(5)} = 0.590 \times 10^6 \text{ lb/in}^2$. $G_{\text{std}}^{(6)} = 0.602 \times 10^6 \text{ lb/in}^2$.

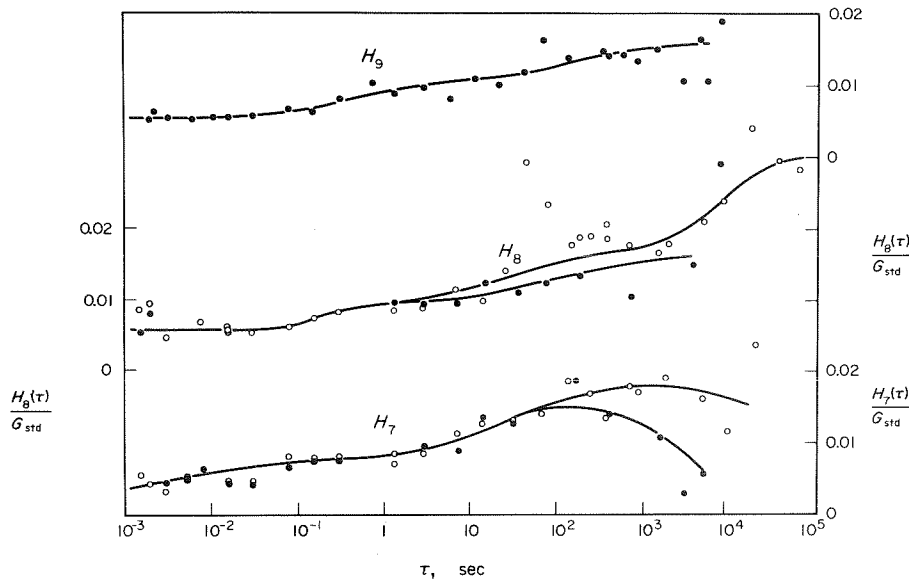


Fig. 3. Comparison of relaxation spectra for wet bovine bone, specimens 7, 8 and 9 (Lakes *et al.*, 1979) in simple torsion; $T = 37^\circ\text{C}$ (first approximation). ● Small strain. ○ Large strain.

observed in scanning electron micrographs to have similar orientations, even in 'intermediate' osteons postulated to have alternating fiber orientations by Ascenzi and Bonucci (1966). Now 'humps' are not discernible in the spectra for bovine bone shown in Fig. 3. It is not clear whether any should be seen, since to the authors' knowledge, no data are available concerning the variation in stiffness among laminae in bovine plexiform bone. It must be recognized that the losses in question are quite small and that the calculation of spectra entails a certain amount of error. As a result, the spectra are 'noisy'; therefore a definitive assignment of mechanisms to the loss in this portion of the time domain cannot as yet be made. Predicted losses in compression for fluid-flow effects can be significant, particularly for large specimens; however, no relevant experimental results are presently available. Loss resulting from piezoelectric-like coupling in dry bone at low frequencies is entirely negligible. Sufficient data are not presently available to assess the losses in wet bone over the full frequency spectrum, due to this effect.

Viscoelastic losses resulting from interfacial (e.g. cement line) motion and from molecular modes in collagen have not been evaluated theoretically. Although some experimental evidence exists which indicates that interlamellar displacements occur over a time-scale which the eye can see, no conclusions can be drawn concerning the resulting relaxation strength. Further experimentation carried out by one of us (R.S.L.), on transient properties of bone over very long times, has shown that extremely large viscoelastic effects occur in bone loaded for extended periods, and that cement-line displacements occur in such specimens.

The observation that collagen alone exhibits viscoelastic behavior is suggestive of a possible role for molecular motions in the collagen phase of bone in determining bone's viscoelastic response. Since most investigators of this behavior in collagen have used material (e.g. rat-tail tendon) which has a structure different from that of bone collagen, the application of such results to the present problem is far from straightforward.

Molecular motions which result in viscoelasticity in polar polymers have been investigated by dielectric relaxation experiments. For wet bone, ionic conduction and interfacial polarization appear to dominate the dielectric behavior (Lakes *et al.*, 1977). Therefore, an alternative approach, such as nuclear magnetic resonance, may be more useful in the experimental investigation of molecular motions in collagen.

Acknowledgements - Contribution 87 from the Laboratory for Crystallographic Biophysics. This research was supported in part by the National Institutes of Health-National Institute of Dental Research, Training Grant 5T1-DE-117-13.

REFERENCES

- Anderson, J. C. and Eriksson, D. (1970) Piezoelectric properties of dry and wet bone. *Nature, Lond.* **227**, 491-492.
- Ascenzi, A. and Bonucci, E. (1966) The compressive properties of single osteons. *Anat. Rec.* **161**, 337-392.
- Bassett, A. (1965) Electrical effects in bone. *Scient. Am.* **213**, 18-20.
- Bassett, A., Pawluk, R. J. and Becker, R. O. (1964) Effects of electric currents on bone *in vivo*. *Nature, Lond.* **204**, 652-654.
- Bur, A. J. (1976) Measurements of the dynamic piezoelectric properties of bone as a function of temperature and humidity. *J. Biomechanics* **9**, 495-507.
- Egan, E., Jr., Wakefield, Z. and Elmore, K. (1951) Low temperature heat capacity and entropy of hydroxyapatite. *J. Am. chem. Soc.* **73**, 5579.
- Evans, F. G. and Bang, S. (1966) Physical and histological differences between human fibular and femoral compact bone. *Studies on the Anatomy and Function of Bones and Joints* (Edited by Evans, F. G.), 142-155. Springer, Berlin.
- Frasca, P. (1974) Structure and dynamical properties of human single osteons. Ph.D. dissertation, Rensselaer Polytechnic Institute, Troy, New York.
- Frost, H. (1960) Measurements of osteocytes per unit volume and volume components of osteocytes and canaliculi in man. *Henry Ford Hosp. med. Bull.* **8**, 208-211.
- Frost, H. (1963) *Bone Remodelling Dynamics*. Thomas, Springfield.
- Hamill, D. and Harper, R. A. (1976) Private communication.
- Hancox, N. (1972) *Biology of Bone*. Cambridge University Press, London.
- Ké, T. (1947) Experimental evidence of the viscous behavior of grain boundaries in metals. *Phys. Rev.* **71**, 533-546.
- Lang, S. (1969) Elastic coefficients of animal bone. *Science, N.Y.* **165**, 287.
- Lakes, R. S., Harper, R. A. and Katz, J. L. (1977) Dielectric relaxation in cortical bone. *J. appl. Phys.* **48**, 808-811.
- Lakes, R. S., Katz, J. L. and Sternstein, S. S. (1979) Viscoelastic properties of wet cortical bone—I. Torsional and biaxial measurements. *J. Biomechanics* **12**, 657-678.
- Liboff, A. and Shamos, M. H. (1973) Solid state physics of bone. *Biological Mineralization* (Edited by Zipkin, I.). Wiley, New York.
- Liboff, A., Shamos, M. H. and deVirgilio, W. (1971). The piezoelectric modulus of bone. Paper Th AM-f3, 15th Annual Meeting, Biophysical Society, New Orleans.
- Marino, A., Becker, R. and Bachman, C. (1967). Dielectric determination of bound water in bone. *Phys. Med. Biol.* **12**, 367-378.
- Mouradian, W. E. (1973). Electrical response of wet bone. M.S. thesis, Massachusetts Institute of Technology, Department of Metallurgy and Materials Science.
- Nye, P. (1957) *Physical Properties of Crystals*. Clarendon Press, Oxford.
- Pfeiffer, B. H. (1977) Local piezoelectric polarization of human cortical bone as a function of stress frequency. *J. Biomechanics* **10**, 53-57.
- Piekarski, K. (1970) Fracture of bone. *J. appl. Phys.* **41**, 215-223.
- Rauber, A. (1876) *Elasticität und Festigkeit der Knochen. Anatomisch physiologische Studie*, p. 75. Engelmann, Leipzig.
- Renton, D. (1970) The viscoelastic properties of bone. M.A. Sc. thesis, University of Waterloo, Waterloo, Ontario.
- Rusch, K. (1965) Dynamic behavior of flexible open cell foams. Ph.D. thesis, Department of Polymer Science, University of Ohio.
- Tischendorf, F. (1951) Das Verhalten der Haversschen Systeme bei Belastung. *Wilhelm Roux Arch. EntwMech. Org.* **145**, 318-332.
- Yoon, H. S. and Katz, J. L. (1976) Ultrasonic wave propagation in human cortical bone, II. Measurements of

elastic properties and microhardness. *J. Biomechanics* **9**, 459–464.
 Zener, C. (1938) Internal friction in solids – general theory of thermoelastic internal friction. *Phys. Rev.* **53**, 90–99.
 Zener, C. (1941) Theory of the elasticity of polycrystals with viscous grain boundaries. *Phys. Rev.* **60**, 906–908.

APPENDIX A

Mechanical Loss due to Piezoelectric and Dielectric Relaxation

Rewriting the constitutive equation (5) and substituting $E_1 = (ij/k'_{11})D_1$,

$$D_1 = \sigma_{ij}d^*_{1ij} + E_1k^*_{11} = \sigma_{ij}d_{1ij} + \frac{ik^*_{11}}{k'_{11}}D_1, \tag{A-1}$$

or

$$D_1 = \sigma_{ij}d^*_{1ij} \left/ \left(1 - \frac{ik^*_{11}}{k'_{11}} \right) \right. = \sigma_{ij}d^*_{1ij} \left/ \left[1 - \frac{i(k'_{11} - ik''_{11})}{k'_{11}} \right] \right. \tag{A-2}$$

$$D_1 = i\sigma_{ij}d^*_{1ij} \tan \delta^{(k)}_{11}, \tag{A-3}$$

where $\tan \delta^{(k)}_{11} = k''_{11}/k'_{11}$ is the dielectric loss tangent. Now since $dD_1/dt = -\omega\sigma_{ij}d^*_{1ij} \tan \delta^{(k)}_{11}$, the following can be written:

$$\int E_1 \frac{dD_1}{dt} dt = \int \frac{\omega\sigma_{ij}d^*_{1ij}\sigma_{kl}d^*_{1kl}}{k'_{11}} \tan^2 \delta^{(k)}_{11} dt. \tag{A-4}$$

The real part of the above expression is the electrical work W_{elec} done in one cycle of sinusoidal deformation. For simplicity, letting $ij = 23, kl = 23$ to remove the implied summations,

$$W_{elec} = \frac{\pi\sigma_{23}^2(d'_{123} - d''_{123})}{k'_{11}} \tan \delta^{(k)}_{11}. \tag{A-5}$$

Now the mechanical work done in one cycle of deformation is

$$W_{mech} = \int_{\text{one cycle}} \sigma_{ij} d\varepsilon_{ij} = \int_0^{2\pi/\omega} \sigma_{ij} \frac{d\varepsilon_{ij}}{dt} dt. \tag{A-6}$$

For a lossy solid, stress and strain are related via the complex compliance

$$S^*_{ijkl} = S'_{ijkl} - iS''_{ijkl},$$

so that for

$$\sigma = \sigma^o e^{i\omega t}, \tag{A-7}$$

$$\varepsilon_{ij} = [S'_{ijkl} - iS''_{ijkl}] \sigma^o_{kl} e^{i\omega t}. \tag{A-8}$$

Then,

$$W_{mech} = \pi\sigma^o_{ij}\sigma^o_{kl}S''_{ijkl}. \tag{A-9}$$

For the shearing stresses considered above, and in a principal coordinate system,

$$W_{mech} = \pi\sigma_{23}^o\sigma_{23}^oS''_{2323}. \tag{A-10}$$

Comparing this with equation (A-5), the electrical contribution to the mechanical loss compliance $\Delta S''$ may be written

$$\Delta S''_{2323} = \frac{d'^2_{123} - d''^2_{123}}{k'_{11}} \tan \delta^{(k)}_{11}. \tag{A-11}$$

Now if the piezoelectric-like coupling is weak, then the storage compliance S' is essentially unchanged, so that

$$\Delta \tan \delta^{Mech}_{2323} = \frac{d'^2_{123} - d''^2_{123}}{k'_{11}S'_{2323}} \tan \delta^{(k)}_{11} \tag{A-12}$$

represents the piezoelectric-like contribution to the mechanical loss for the geometry under consideration.

Note added in proof – Experimental evidence for inhomogeneous motion at the cement lines as a dominant mechanism for long term time-dependent deformation in bone has been published recently by one of us (R.S.L.): Lakes, R. S. and Saha, S. (1979) Cement line motion in bone. *Science, N.Y.* **204**, 501–503.

